PRODUCTION OF HIGH PURITY SILICA BY MICROFLUIDIC-INCLUSION FRACTURE USING MICROWAVE PRE-TREATMENT

A.J. Buttress [a], J.M. Rodriguez, A. Ure, R.S Ferrari, C. Dodds, S.W. Kingman.

Advanced Materials Research Group, Faculty of Engineering, University of Nottingham, NG7 2RD, UK.

[a] - corresponding author Adam Buttress: adam.buttress@nottingham.ac.uk

ABSTRACT

Demand for high purity silica used in component manufacture is set to outstrip current supply in the near future. As such, alternative processing routes to feed-stock materials suitable for use in lighting and solar cell fabrication are required, without having to rely on reject material from semi-conductor manufacture. In this work, we report a facile, environmentally friendly method of producing quartz powder with a total residual impurity level of 30 ± 3 ppm from whole pebbles having an initial impurity level of 158 ± 22 ppm. This has been achieved using a metallurgical upgrading process incorporating microwave pre-treatment, crushing and milling, High Intensity Wet Magnetic Separation (HIWMS) and acid leaching. This process yielded a quartz powder having an 80% reduction in residual impurities compared to the untreated quartz pebbles. Pre-treatment of whole quartz pebbles in a multimode microwave cavity for 10 minutes yielded a reduction of the residual elemental impurity content associated with micro-fluidic inclusion sites containing calcium, potassium and sodium of 84, 78, and 50 % respectively. Statistically significant reduction in residual aluminium phases was also observed (83%) compared to the as received material to below the IOTA® specification for Ultra High Pure Quartz produced by Sibleco. Mechanistically, this has been achieved by selectively heating impurity containing micro-fluidic inclusion sites. Resulting in their explosive decrepitation and enabling removal of the impurities in subsequent processing steps. It has been concluded that natural quartz pebbles can be upgraded through a combination of microwave treatment, magnetic and chemical refinement to produce a viable feedstock for the subsequent production of solar grade silicon.

Keywords: Silica; Microwave Processing; Micro-fracture

1. INTRODUCTION

Increasing global energy demands coupled with ambitious carbon reduction targets have served as the key drivers for the development of clean energy technologies (Lynch, 2009). Photovoltaics (PV), which collect solar energy and convert

it to electricity have played, and will continue to play a strategic role in these green technologies into the future. Silicon based PV cells still accounted for 90% of total PV sales in 2011, with average annual growth rates in excess of 40% over the last two decades (Frankl et al., 2010). The principal commodity in the supply chain of the photovoltaic industry is reject material from the semi-conductor industry. However, it has recently been recognised that supply from this source has become a critical issue, driving up feedstock prices and limiting expansion of industrial production (Drouiche et al., 2014). As such, much effort is currently being directed towards developing technologies for utilising alternative sources for the production of Solar Grade Silicon (SoG). While there are no defined specifications for this material, the industry standard is currently set by the company Sibelco, a subsidiary of Unimin Corp, whose product known as IOTA Quartz has a total contaminant levels of 20ppm (Hughes, 2013). Typical product specifications for this material are reported in (Kogel, 2006). The pre-curser material is normally metallurgical-grade silicon which has a typical specification of 98.5 – 99.5% Si[13] (Xakalashe and Tangstad, 2012) and whose current production is on the order of millions or tonnes per year at relatively nominal cost (Pizzini, 2010).

Naturally occurring quartzite deposits are normally mined as the raw material for these applications. Impurities typically reside in microfluidic inclusions; mineral associations (such as rutile TiO_2) in the bulk material (Götze et al., 2004) and as ionic substitutions within the crystalline lattice of the quartzite itself (Santos et al., 2015). Current industrial technologies for production of metallurgical grade silicon involve carbothermic reduction of silicon dioxide at 1500 - 2000°C in an electric arc furnace (Pizzini, 2010). This material is then upgraded to solar grade silicon using the so-called Siemens process (referred to as the chemical upgrading route), which firstly involves the production of a trichlorosiline via a gasification reaction between silicon and hydrochloric acid. Silicon is then produced through deposition by reduction under a hydrogen atmosphere in a Siemens reactor. This is an energy intensive process (>100kWh/kg) characterised by typically low yields (Xakalashe and Tangstad, 2012). The metallurgical upgrading route is known to be less energy intensive and has a lower environmental impact, although this only accounted for <8% of total solar grade silicon production in 2008 (Xakalashe and Tangstad, 2012). It involves a series of processing steps which can include mechanical separation (Delannoy, 2012), vacuum refining, acid leaching, plasma purification (Safarian et al., 2012) and directional solidification (Sarti and Einhaus, 2002). More recently, production of polysilicon in a Fluidised Bed Reactor (FBR) has been described using saline gas as the feedstock. This process uses less energy than the Siemens process by an order of magnitude, although only 10% of global polysilicon is produced by this method, owing to the relative immaturity of the technology (Bye and Ceccaroli, 2014). The market share of solar grade silicon produced via the metallurgical route could be increased by reducing manufacturing costs through the development of more sustainable processing techniques with lower environmental impacts.

1.1. BASIS FOR UPGRADING QUARTZ THROUGH MICROWAVE TREATMENT

Microwave heating has established itself as an enabling technology. It is characterised by rapid, volumetric and when used to treat multiphase materials - selective heating. As such, it has found use in industrial sectors as diverse as mineral processing (Ali and Bradshaw, 2011; Amankwah et al., 2005; Batchelor et al., 2016), environmental remediation (Jones et al., 2002; Junior et al., 2015), oil recovery (Shang et al., 2006), pre-processing of carbonaceous fuels (Marland et al., 2000) and chemical synthesis (Kappe and Dallinger, 2006; Kitchen et al., 2013). Previous characterisation work (unpublished report) on the feedstock quartz used in this work has shown it to be relatively pure (99.9950%). Characterisation of the untreated sample by Scanning Electron Microscopy with Energy Dispersive X-ray Spectroscopy (SEM-EDS) and proton microprobe has shown contaminants to largely reside in fluidic micro-inclusions within the bulk quartz matrix.

Fluid inclusions are micron-scale cavities which contain paleo-fluids physically trapped within mineral grains in crystal lattice imperfections, in structural holes or channels, or along grain boundaries (Roedder and Ribbe, 1984). Fluid inclusions in quartz predominantly occur in three different forms, as monophase fluid only inclusions, dual-phase inclusions which contain fluids and a vapour or solid component, or multi-phase inclusions containing fluid, vapour and solid components(Bodnar, 2003; Roedder and Ribbe, 1984).
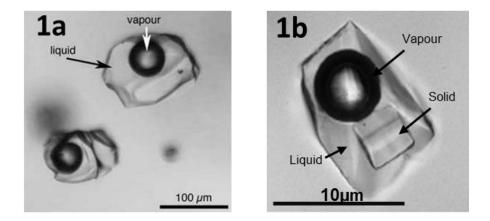

Figure 1: Example images illustrating types of fluid inclusions. (1) dual-phase liquid and vapour inclusions; (2) a multi-phase liquid, vapour and solid inclusion. (Kendrick and Burnard, 2013)

Fluid inclusions in quartz originate from hydrothermal geological processes during deposition, or through subsequent alteration events and changes in pressure and temperature conditions (Bodnar, 2003). The predominant elemental composition of the fluidic component of the inclusions is an ionic solution consisting of water (H_2O) with variable concentrations of potassium, sodium and chloride. Vapour phases are commonly present as CO_2, CH_4 or N_2, while solid phases are predominantly halite (NaCl) or sylvite (KCl) (Roedder and Ribbe, 1984).

When a fluid inclusion contained within a mineral grain is heated it may rupture or decrepitate. Decrepitation refers to the process by which the heating and subsequent increase in internal pressure of a fluid inclusion exceeds the confining pressure of the surrounding mineral grain. Once the confining pressure is exceeded, the inclusion will irreversibly rupture and crack the surrounding grain or rock, releasing or leaking the contained fluids or gases. Fluid inclusion decrepitation events can be partial, with an incomplete release of inclusion contents, total, or explosive, which result in pits or cavities to be formed in the sample. The temperature of decrepitation of fluid inclusions in quartz is controlled by a number of parameters, including inclusion size, shape, composition and the characteristics of the host mineral grain. Thermally induced mechanical decrepitation of fluid inclusions in quartz has been shown to occur initially at temperatures of <600°C (Barker and Robinson, 1984), with a second stage occurring between 1200-1450°C (Kendrick et al., 2006). The initial stage shows decrepitation occurring between ~150°C to ~500°C, with a decrepitation peak (the dewatering peak) occurring at ~573°C which is the temperature of α-β quartz inversion, where quartz changes from trigonal to hexagonal crystal structure and reduces in density (Barker and Robinson, 1984). A second stage of decrepitation (the degassing peak) occurs between ~1200°C to ~1450°C during transformation of β-quartz to cristobalite (Kendrick et al., 2006).

The propensity for a material to be heated in an electromagnetic field is defined by its dielectric properties. The dielectric constant is a measure of a materials ability to store electromagnetic energy. The loss factor is a measure of a materials ability to dissipate absorbed electromagnetic energy as heat. The higher the loss factor, the better the material will heat in an applied microwave field. Table 1 shows the dielectric properties for some relevant materials.

Table 1: Dielectric properties of materials common to quartz pebbles at 2.45GHz and 25°C (Metaxas and Meredith, 1983)

Material	Dielectric Constant (ε')	Dielectric Loss (ε'')
Quartz	4.0	0.0001
Water	77	13
0.3M Sodium Chloride Solution	70	17

It can be seen from the table that quartz itself has a very low loss and so essentially transparent to microwave energy, while the sodium chloride solution has a loss many orders of magnitude higher, so will heat strongly in an applied field. As a result of these widely differing dielectric properties, when the quartz pebbles are exposed to microwave energy of sufficient intensity, a selective heating effect is expected to occur. This could then result in targeted heating of the

microfluidic inclusions, while the bulk quartz remains relatively cold. In this case, it may result in targeted decrepitation events and explosive fracture within the inclusion zones, then enabling subsequent processing steps to yield a refined quartz with reduced residual levels of trace contaminants. This mechanism of differential thermal expansion has been shown to yield significant process benefits in the treatment of mineral ores (Batchelor et al., 2015).

The aim of this work is to investigate if the selective heating effect can be utilised in a microwave pre-treatment step to upgrade naturally occurring quartz pebbles by enhancing the removal of impurities associated with micro-fluidic inclusions, containing the elements aluminium, sodium, calcium and potassium.

2. EXPERIMENTAL PROGRAMME

The experimental programme was divided into a sample pre-characterisation stage, followed by four experimental stages each comprising of the following steps - microwave treatment, size reduction, Wet High Intensity Magnetic Separation (WHIMS), chemical leaching and analysis. Initial microwave treatment used a multimode cavity for treating batches of quartz placed in its base. After treatment, the quartz pebbles were resized using a jaw crusher and planetary ball mill. The fine powders were then subject to magnetic separation and chemical leaching using either acid or water. Residual contaminant levels were quantified by Inductively Coupled Plasma Atomic Absorption Spectroscopy (ICP-AES), using a Varian Vista-Pro Inductively Coupled Plasma - Optical Emission Spectrometer. Solid samples were first digested in a mix of hydrofluoric, perchloric and nitric acid.

A second round of multimode tests was then undertaken with the multimode cavity using a microwave transparent ceramic crucible and silica flour which was used an insulator to minimise heat loss from the samples. Also trialled was treatment in a Radio Frequency (RF) tunnel. Again these samples were subject to the same subsequent processing steps. Evaluation of the final product was again undertaken using ICP-AES, in addition to qualitative SEM-EDS studies to evaluate the effect of the treatment on any microfluidic inclusions, supported by optical analysis of thin sections taken from the treated whole pebbles.

To investigate if the final purity of the processed quartz powder could be improved, the effect of more aggressive leaching conditions was evaluated on samples remaining from the magnetic separation step from the previous work.

Finally, powders derived from the magnetic separation step of quartz pebbles treated in the optimised multimode cavity were retreated in a single mode microwave system. These were then subjected to the most effective chemical leaching

(in terms of reduction in residual contaminant levels) procedure taken from the previous stage. The structure of the experimental programme is presented in Figure 2. It is split into four stages:

- Stage One – initial trials in a multimode microwave cavity; followed by sizing to 75 - 300µm; WHIMS; then each sample mass split in two; one half leached with hydrochloric acid and the other half with water

- Stage Two – optimised trials of separate samples in a multimode microwave cavity (using a crucible and silica packing) or Radio Frequency tunnel; then size reduction; WHIMS and leaching with hydrochloric acid

- Stage Three – quartz powder originating from the 2nd stage multimode tests (after WHIMS) were subjected to a more aggressive leaching procedure – ca.3% HF or reflux with 7m HCl

- Stage four – again quartz powder originating from the 2nd stage multimode tests (after WHIMS), were retreating in a single mode microwave cavity, then leached with ca. 3% HF

A detailed description of the methods used in each stage of the experimental program is given in the next section.
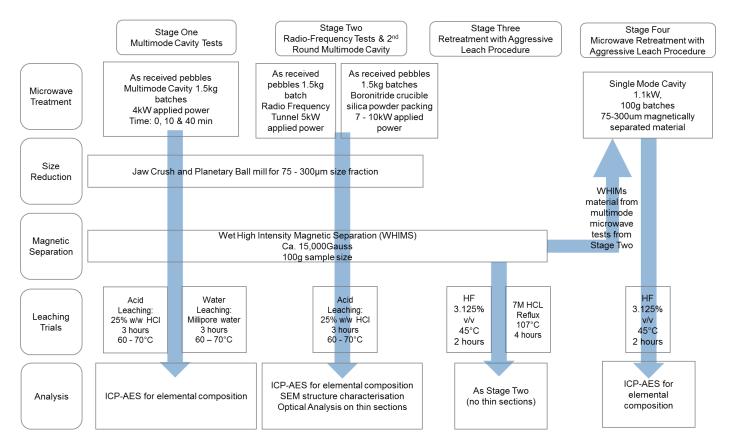

Figure 2: Overview of the four stages comprising the experimental programme

2.1. METHODS

Pre-characterisation of impurities present within the quartz was conducted using a combination of optical microscopy and SEM-EDS. Optical analysis of untreated material was conducted under transmitted light using a Leica M205

automated stereomicroscope with a 5 mega pixel digital camera on particulate sample grain mounts (+75-300µm) and Petrographic Thin Sections (PTS) of whole quartz pebbles (-15mm, +15mm-26.5mm, +26.5mm pebbles). The thin sections were prepared by impregnating the samples with clear epoxy resin, which were then cut to size, flattened and stuck to object glasses before being ground to 40-50 µm thickness on a Pelcon Automatic Thin Section Machine. The sections were then polished on a Buehler EcoMet 300 Grinder-Polisher and finished at a thickness of approximately 30 µm. The polish was achieved by using 3 µm and 1 µm diamond suspensions on perforated and felt cloths respectively. The analysis was conducted in order to qualitatively assess the characteristic size and morphology of fluid inclusions present within the quartz, and to investigate the spatial distribution of inclusions within the quartz pebbles. SEM-EDS analysis was conducted using a FEI Quanta 600 Scanning Electron Microscope (SEM) with dual Bruker XFlash® 5030 EDX detectors and Mineral Liberation Analyser (MLA) automated mineralogy software. Quartz samples were prepared for SEM-EDS analysis as carbon coated 30mm resin-mounted polished sections produced from crushed and milled particulate samples (+75-300µm). Qualitative and semi-quantitative EDS analysis was conducted using Bruker Esprit® microanalysis software for the collection of EDS spectra, EDS line scans and elemental sample surface mapping. Impurities analysed using this method represent surface, or near-surface features, that occur within the range of the interaction volume of the electron beam within the samples (~ 5µm depth from surface). Analysis by ICP-OES was undertaken using a Varian Vista-Pro spectrometer, on diluted solutions derived from digestion in a mix of hydrofluoric, perchloric and nitric acid of 2.0g samples of the quartz powders.

In stage one, microwave treatment used a multimode cavity coupled to a 15kW microwave generator operating at 2.45GHz. Impedance matching was achieved using a 3-stub autotuner in the transmission line. 1.5kg batches of material placed on the base of the cavity were subject to three treatment regimens corresponding to the maximum microwave power that could be applied and coupled into the load. A power of 4kW was applied to the multimode cavity for 40 10; and 0 minutes (untreated control). Each treatment was repeated in triplicate. Every 2 ½ min, the samples were turned by hand with a spatula so as to ensure even treatment of the whole batch. These samples were then jaw crushed to <5mm and planetary ball milled inside a ceramic lined pot to a produce a 75 – 300um size fraction. This is considered the optimum size fraction for the production of solar grade silicon. The fine material was subsampled to 100g, then subjected to high intensity wet magnetic separation (HWIMS) to remove magnetic and paramagnetic material at a magnetic field strength of at least 15,000 Gauss. Finally, initial leaching trials were conducted using a moderate strength HCl solution (25% w/w) and high purity water for comparison, in a solids to liquid ratio of 40:100 with stirring for 3 hours at a temperature of 60 - 70°C, in a three-necked round bottom flask. After cooling, the solids were filtered under vacuum and washed with successive volumes of Millipore water until the washings were pH>6. Analysis of the final quartz was then undertaken by ICP-AES using the digestion procedure described previously for the following elements: Al; Ca; Cr; Fe; K; Na; and Ti.

Stage two work focussed on optimising the microwave treatment regime in the multimode cavity by using a ceramic crucible made from boronitride. 1.1kg batches of quartz pebbles were blended with 400g silica flour into the crucible and placed on the rotating plinth of the cavity. In this configuration, the applied power could be increased from 4kW to 7 - 10kW. Four separate microwave treatments were undertaken. Each targeting the maximum applied power for the longest processing time. The end of the test was taken to be when the reflected power increased to >10% forward power. This was taken to correspond to removal of the absorbent phases (principally the inclusion fluid). The treated pebbles were then washed in Millipore water to remove the silica flour and dried in the oven at 105°C.

At lower frequencies, the ionic loss mechanism makes the dominant contribution to the heating effect (Metaxas and Meredith, 1983). It then follows that treatment using energy at lower frequencies will enhance the selective heating effect at fluid inclusion sites. As such, in addition to the microwave tests, a 1.5kg sample of the feedstock pebbles was treated in a Sariem TRF radio frequency system operating at 27.12 MHz. The pebbles were placed on ceramic wool either side of 2 × 2kg of quartz sand (to enable impedance matching) with a second layer of ceramic wool over the top. A forward power of 5kW was then applied for 8 minutes. After cooling, all five treated samples were then subjected the same size reduction and magnetic separation procedures as stage one. Leaching tests were then undertaken using the procedure already described using hydrochloric acid. Analysis of the final refined quartz powders was then undertaken by ICP-AES as previously described, and finally qualitative SEM-EDS to evaluate the effect of the treatment procedures on the microstructure of the material. Complimentary petrographic thin sections of the whole untreated and treated pebbles were also prepared from sizes -15; +15-26.5 and +26.5 mm and analysed under an optical microscope to visually assess the impact of the treatments on the characteristics and distribution of fluid inclusions in the samples.

In stage three, the three of the previous samples (two microwave and one RF treated) processed up to the magnetic separation step were treated under more aggressive leaching conditions. The samples were split in two, for each, half the subsample was then further reduced to 40g and leached with 60g of 3.125% hydrofluoric acid solution in a PTFE crucible for 3 hours with warming in a water bath at 45°C. After cooling, the samples were vacuum filtered and washed with successive volumes of Millipore water before drying in the oven at 105°C. The remaining half of the magnetically separated sample was subsampled to 100g and refluxed in a round bottom flask at 107°C with 7M hydrochloric acid solution and stirring for 4 hours. Following cooling, the solid was vacuum filtered and washed with successive volumes of water until the pH of the washing was pH>6. Analysis of the final treated products was undertaken by ICP-AES and SEM-EDS as previously described.

The final stage took the two samples not subjected to retreatment by aggressive leaching and processed them again using a microwave single mode cavity. This type of cavity is characterised by supporting a single spatially well-defined area of high electric field propagating at one frequency or mode within it. At 2.45GHz, they are therefore smaller than a

multimode cavity, but enable the heating effect to be focussed in the sample without the use of a turntable. For these tests, 100g of each sample was placed in a boronitride crucible and treated with microwaves at a power of 1.1kW generated from a Sariem 2kW generator operating at 2.45GHz. Matching was achieved using a combination of a variable position piston short at the terminating end of the waveguide and a 3-stub automatic tuner in the transmission line itself. Analysis of the final treated products was undertaken by ICP-AES.

3. RESULTS AND DISCUSSION

3.1. CHARACTERISAION OF THE QUARTZ PEBBLES

The as received pebbles generally fell into the -10+75mm size fraction. Analysis by AES-ICP revealed that the pebbles had the composition presented in Table 2.

Table 2: Elemental Composition of the as received quartz pebbles by AES-ICP

Elemental Composition (ppm)							
Element	Al	Ca	Cr	Fe	K	Na	Ti	Total
Head grade	102 ± 14	6 ± 4	<0.3	11 ± 1	9 ± 2	18 ± 1	12 ± 1	158 ± 22

The results of the optical analysis of thin sections made from untreated quartz is presented in Figure 3 showing the occurrence, distribution and morphology of the fluid inclusions. They generally occurred either as large ~10 – 30µm inclusions ranging in shape from round to elliptical or irregular (Figure 3a), or as clusters or seams of fine (2-5µm) and ultra-fine (<2µm) inclusions giving the quartz a cloudy appearance (Figure 3b). Also observed were fine-grained (<~20µm) iron oxides distributed through the quartz matrix (Figure 3c).
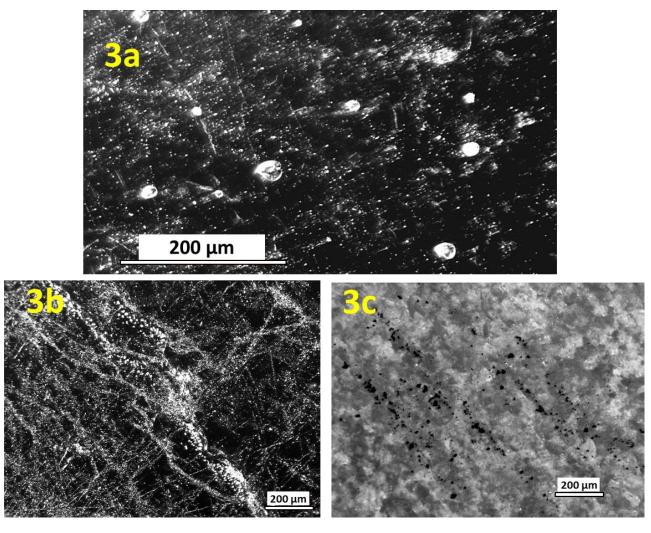
Figure 3: Optical images collected from thin sections prepared from the as received quartz pebbles. (3a & 3b) show the distribution of fluid inclusions through the quartz; (3c) shows opaque impurities (attributed to Fe-oxides) Note: dark areas are voids from partially opened inclusion sites.

SEM-EDS analysis of the -75-300um powdered untreated material was undertaken to investigate the occurrence and distribution of impurities within the sample. As SEM-EDS is a 2D surface analysis technique, inclusions and impurities were required to be on or very near (<~5μm) the sample surface in order to be analysed by EDS. In order to attempt to locate intact near surface inclusions, an initial mineral map was collected using the Mineral Liberation Analyser (MLA) automated mineralogy capability of the SEM. A customised mineral list was applied to identify areas within the quartz grains where the interaction volume of the electron beam within the grain, intersected a volume of the quartz that indicated the presence of an elevated sodium concentration. This produced a sodium 'hot spot' map where inclusions could be found near the surface of the sample mount for further analysis with element mapping, element line scans and collection of x-ray spectra. The results are shown in Figure 4. The analysis indicates that the fluid inclusions distributed throughout the quartz matrix are rich in elemental sodium that can be attributed to dissolved halite. This ionic solution would be expected to heat readily when exposed to microwave energy (see Table 1).
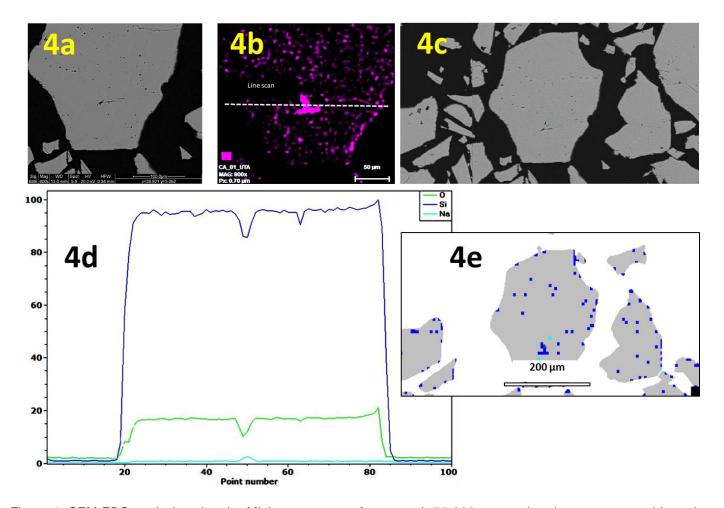
Figure 4: SEM-EDS analysis using the MLA programme of untreated -75-300um powdered quartz mounted in resin. (4a) target grain for analysis; (4b) BSE image of grains on mount surface elemental map of sodium showing fluid inclusion (4c) BSE image of grains on mounted surface (4d) results of line scan across indicated area; (4e) Sodium map produced via MLA revealing spatial distribution of fluid inclusions

3.2. STAGE ONE - MULTI-MODE TESTS

The as received quartz pebbles were arranged in the base of the multimode cavity as shown in Figure 5. It was noted after treatment that a proportion of the pebbles had fractured into smaller particles. This is attributed to explosive fracture along inclusion seams within susceptible particles. The energy dose delivered to the samples was 0; 0.45 and 1.78 kWh/kg, corresponding to treatment times of 0 (untreated control); 10 and 40 minutes. The untreated pebbles had a milky opaque appearance which changed to discoloured white on microwave treatment.
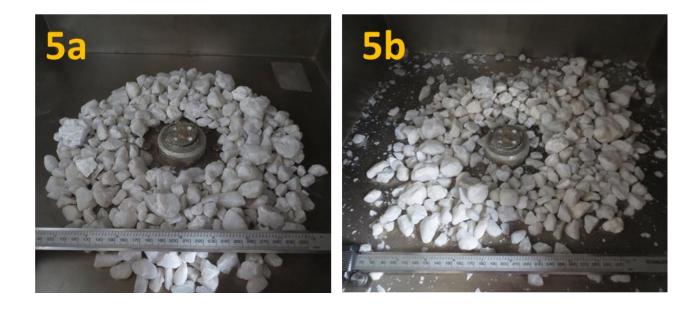
Figure 5: Quartz pebbles arranged on the base of the multimode cavity before (5a) and after (5b). Note the fracture of pebbles into smaller fragments after treatment

The final elemental composition of the product quartz powders after being subject to microwave treatment, size reduction, magnetic separation and leaching is shown in Table 3. The whole pebbles were processed without microwave pre-treatment to evaluate the effect of crushing grinding, magnetic separation and leaching steps alone. Separate samples of whole pebbles were subject to treatment for 10 and 40 minutes in the multimode cavity, then subject to size reduction, magnetic separation. The samples were split and half was leached in water and the remainder leached in HCl. It can be seen that overall, acid leaching was more effective and yielded residual contaminant levels of around 10ppm less than water for equivalent microwave treatment time. Microwave treatment resulted in a 10ppm drop in total residual contaminants compared to the untreated control set. Analysis of the values based on a t-test at 90% confidence level showed that the reduction in aluminium (T_{10min} 67%, T_{40min} 65%) and sodium (T_{10min} 41%, T_{40min} 31%) content was statistically significant compared to the untreated control set. This reduction is primarily expected to be resulting from the post-microwave treatment steps (see section 4). As previously described, sodium principally resides within the fluid inclusions of the quartz, which is preferentially heated by microwaves. Aluminium tends to occur as cationic substitutions within the quart lattice itself and as solid phases occurring primarily as feldspars along grain edges. The reduction in Al content on microwave treatment could be the result of differential thermal expansion of the feldspars causing microwave-fracture along the gain boundaries and separation of the feldspar from the quartz grains. Significant is the fact that treatment for 40 min, equivalent to an energy dose of ~1.8kWh/kg, was no more effective at ultimately reducing the levels of residual contamination than treatment for 10 min (0.45kWh/kg). It suggests that the mechanistic effect which upgrades the quartz occurs only within the first 10 min of treatment. This could well correspond to explosive failure of the microfluidic inclusions causing microfractures to the gain surface, thus enabling subsequent processing steps to remove exposed contaminant phases. Once an inclusion has decrepitated, further exposure to microwave does not

cause in any additional damage to the quartz matrix and ultimately no further reductions in residual levels of contamination is observed. Overall microwave treatment yields a 25% reduction in contaminant levels in the final quartz products compared to the control set (T_{0min}) subjected to equivalent subsequent metallurgical processing steps.

Table 3: Elemental composition of stage one multimode cavity tests by ICP-AES of digested final product quartz powders after water and acid leaching

Sample ID	Leach Conditions	Elemental Composition (ppm)							
		Al	Ca	Cr	Fe	K	Na	Ti	Total
Head Grade	None	102 ± 14	6 ± 4	<0.3	11 ± 1	9 ± 2	18 ± 1	12 ± 1	158 ± 22
T_{0min}	Water 60-70°C	24 ± 1	3 ± 0.2	<0.3	7 ± 0.4	4 ± 1	13 ± 1	3 ± 0.2	53 ± 3
T_{10min}		24 ± 1	3 ± 0.2	<0.3	7 ± 0.4	4 ± 1	13 ± 1	3 ± 0.2	53 ± 3
T_{40min}		17 ± 1	3 ± 1	<0.3	5 ± 0.3	3 ± 1	10 ± 1	4 ± 1	41 ± 3
T_{0min}	25 % w/w HCl 60-70°C	18 ± 3	1 ± 0.1	<0.3	3 ± 0.1	3 ± 1	12 ± 1	3 ± 1	41 ± 6
T_{10min}		13 ± 3	1 ± 0.1	<0.3	2 ± 0.1	2 ± 0.1	9 ± 1	3 ± 1	30 ± 4
T_{40min}		12 ± 1	1± 0.1	<0.3	2 ± 0.1	2 ± 0.1	10 ± 1	3 ± 1	30 ± 3

Note: reported error is derived from the standard deviation of the triplicate analysis of each sample or 5% of the mean value of the triplicate analysis if all three results were the same, whichever is greater

Optical analysis taken from powered T_{10min} mounted in resin blocks is shown in Figure 6. The images show the resulting microstructure of the quartz following an explosive decrepitation of a fluid inclusion. It can be seen that these regions have a roughly circular and apparently expanded shape, some with a clarified appearance round their outer edge (6a and 6c). These regions appear to be surrounded by rings or clusters of fluid/vapour debris most likely caused by the explosive decrepitation event. It is suggested that following explosive failure of a fluidic inclusion, if the failure is still contained wholly within the bulk structure of the quartz grain, dissipation of the localised internal pressure causes the diffusion and deposition of the contaminants around the rim of the inclusion. This is another possible explanation as to why contaminant levels of 30ppm may persist in the stage one trial batches of the processed quartz.
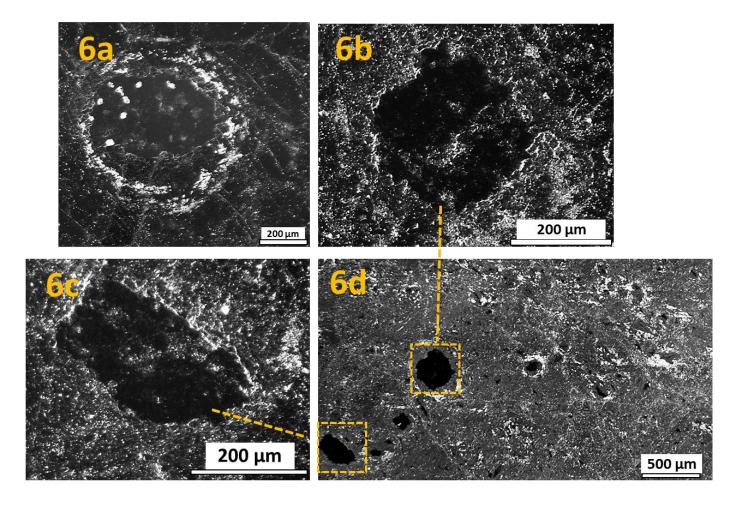
Figure 6: Optical analysis of resin mounted blocks of powered microwave treated sample T_{10min}, showing the microstructural changes in the quartz gains resulting from decrepitation of fluid inclusions. Note deposition of inclusion debris around the edge of a decrepitation site (6a). Irregular shaped voids resulting from decrepitated inclusion sites (6b and 6c). The same decrepitation sites shown within the wider microstructure of the quartz (6d).

3.3. STAGE TWO – OPTIMISED MULTI-MODE TESTS

A characteristic property of multi-mode cavities is that they support a number of propagating modes (dominant frequencies) which can constructively or destructively interact with each other (Metaxas and Meredith, 1983). This results in a non-homogenous distribution of electric field intensity within it. To compensate for this effect, such cavities often incorporate turntables to move the material though the field or mode stirrers to constantly change the field pattern to increase the uniformity of treatment. The initial tests had the quartz arranged in a static position on the floor of the cavity. While the material was turned over at regular intervals during microwave treatment, the electric field strength tends to zero at the cavity walls. In order to enhance the upgrading of the quartz pebbles through microwave treatment, targeted failure of fluid inclusions could be enhanced by increasing the electric field intensity the material is exposed to. In the optimised tests, this was done by holding the quartz in a boron nitride ceramic crucible on the turntable of the

cavity and using silica flour which was used as a thermal insulator to minimise radiative heat losses. In this configuration, the quartz is held in the approximate centre of the cavity where the electric field strength is expected to be higher than at the cavity floor. It was also constantly rotated though the field, to increase the uniformity of treatment. By also using silica flour, the power applied could be increased from 3-4kW (sighter tests), to 7- 10kW in the optimised trials, before the reflected power increased indicating the end of the test.

For each multimode cavity test, the highest power for the maximum treatment time was applied. The end of the run was indicated by an increase in process arcing within the cavity. This occurs when the electric field strength within the cavity exceeds the breakdown voltage of air. It results in an electrical discharge from one point in the cavity to another. In this case it is associated with a drop in absorbed energy by the quartz, possibly due to the absorbent fluid phases being driven off by the heat evolved in the test samples. For the RF test, the system described in (Ferrari-John et al., 2016) was used. The treatment regimes for each of the optimised tests and elemental composition of the final processed quartz is shown in Table 4. After microwave or RF treatment, each sample was subjected to size reduction, magnetic separation, and HCl leaching only, as the previous tests showed that HCl was a more effective leaching procedure than water.

Table 4: Treatment regimes and final product composition of quartz processed with optimised microwave and RF conditions and analysed by ICP-AES after acid decomposition

Sample ID	Max Power kW	Time mm:ss	Energy Dose kWh/kg	Elemental composition (ppm)							Total ppm
				Al	Ca	Cr	Fe	K	Na	Ti	
M_1	7	01:52	0.12	24 ± 1	1 ± 0.1	0.1	2 ± 0.2	5 ± 0.3	10 ± 0.5	2± 0.1	44 ± 2
M_2	10	04:48	0.50	23 ± 1	2 ± 0.2	<0.1	2 ± 0.1	4 ± 0.1	10 ± 0.5	2 ± 0.1	43 ± 2
M_3	8	04:48	0.48	25 ± 1	2 ± 0.2	<0.1	2 ± 0.1	3 ± 0.3	10 ± 0.5	2 ± 0.1	44 ± 2
M_4	10	04:02	0.38	26 ± 1	2 ± 0.1	<0.1	2 ± 0.1	4 ± 0.1	10 ± 0.5	2 ± 0.1	45 ± 2
RF_1	5	08:00	0.24	27 ± 3	1 ± 0.2	<0.1	2 ± 0.1	3 ± 0.2	10 ± 0.5	1 ± 0.1	44 ± 3

Using the optimised treatment regimes, the level of total residual contamination was actually higher (~15ppm) than T_{10min} and T_{40min} samples, which were leached with HCL from the earlier tests. This is a result of having generally higher aluminium. This is considered further in section 4.

However, residual sodium levels were about 2ppm lower across the samples tested. The effect of RF treatment yielded no significant change in contaminant levels compared to the microwave treated set. To investigate why no enhancement of contaminant removal was found overall, despite using an improved treatment regime at higher power, thin sections prepared from the whole treated pebbles which were analysed to characterise any change in the microstructure of the quartz, and in particular, residual fluidic inclusions. Example analysis of sample M_1 is shown in Figure 7. Minimal intact fluid inclusions were found following microwave treatment. Those that remained, tended to reside towards the edges and surfaces of the particles. The shape of those remaining had also changed from largely spherical to elongated. This may be attributed to the residual inclusion fluid being forced through line fissures and other lines of weakness within the quartz matrix.
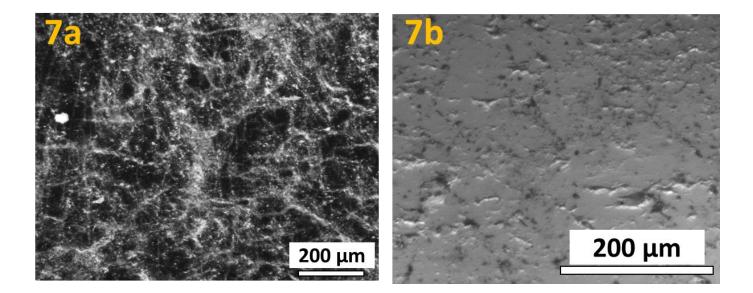

Figure 7: Optical analysis of thin sections prepared from microwave treated (M_1) pebble showing inclusion fluid deposited through grain boundaries and fractures (6a); and (6b) fractured elongated remnant inclusion sites

3.4. STAGE THREE – AGGRESSIVE LEACH CONDITIONS

It has been shown that the samples subjected to the optimised multi-mode microwave and RF treatments exhibited significant micro-structural damage as a result of rupture at fluid inclusion sites, but that fluid appeared to have been deposited within grain boundaries; cleavage planes and fractures. Selected samples from the previous set (M_1, M_4 & RF_1) were then retreated under more aggressive leaching conditions – boiling 7M HCl and 3% (w/w) HF at 45°C, to determine if the remaining impurities could be removed (Table 5)

Table 5: ICP-AES elemental analysis of stage three samples retreated under more aggressive leach conditions

Sample ID	Leach Conditions	Elemental Composition (ppm)							
		Al	Ca	Cr	Fe	K	Na	Ti	Total
M_1	7M HCL, 107°C	27 ± 1	0.7± 0.1	<0.3	2 ± 0.1	3 ± 0.2	11± 0.5	3 ± 0.2	46 ± 2
M_4		23 ± 1	0.6± 0.1	<0.3	2 ± 0.1	4 ± 0.2	10± 0.5	2 ± 0.1	41 ± 2
RF_1		23 ± 1	0.6± 0.1	<0.3	2 ± 0.1	3 ± 0.2	11± 0.5	2 ± 0.1	40 ± 2
M_1	3% HF, 45°C	20 ± 1	2 ± 0.1	<0.3	4 ± 0.2	4 ± 0.2	10± 0.5	2 ± 0.1	40 ± 2
M_4		17 ± 1	2 ± 0.1	<0.3	2 ± 0.2	4 ± 0.2	10± 0.5	2 ± 0.1	37 ± 2
RF_1		18 ± 1	1 ± 0.1	<0.3	3 ± 0.2	4 ± 0.2	9± 0.5	2 ± 0.1	37 ± 2

Retreating the quartz with boiling concentrated HCL results in a marginal drop in total contaminant levels for samples M_4 and RF_1 (~4ppm) due to a drop in aluminium and sodium, but essentially no change in M_1. Re-leaching using HF was more effective, resulting in a drop of around 8ppm in total contamination (18%) for M_4. It is suggested that the HF leach procedure is more effective at removing Al which resides as lattice substitution impurities within the quartz itself, when they are on the near surface of the material exposed to the leach solution. This is why an average reduction in residual Al contamination of 8ppm is observed when the same samples are leached with HF compared to boiling HCl.

Little change by either procedure affected the final sodium content nor that of the other elements evaluated in the analysis. This suggests that the previous, less aggressive leach procedure, was effective at removing contaminants residing on the surface or in fractures accessible to the leach solution. Residual contaminants then remained locked within the matrix of the quartz. This is evident by SEM-EDS analysis. Overall, the samples M_1 – M_4 showed no qualitative differences in either composition nor microstructure differences were found. In RF_1, as previously described, a greater degree of explosive decrepitation was observed. Example Analysis is shown in Figure 8 of sample M_4. This shows a solid iron-rich inclusion mineral that has been exposed on the surface of the resin block by the necessary grinding and polishing which had persisted within the sample after treatment.
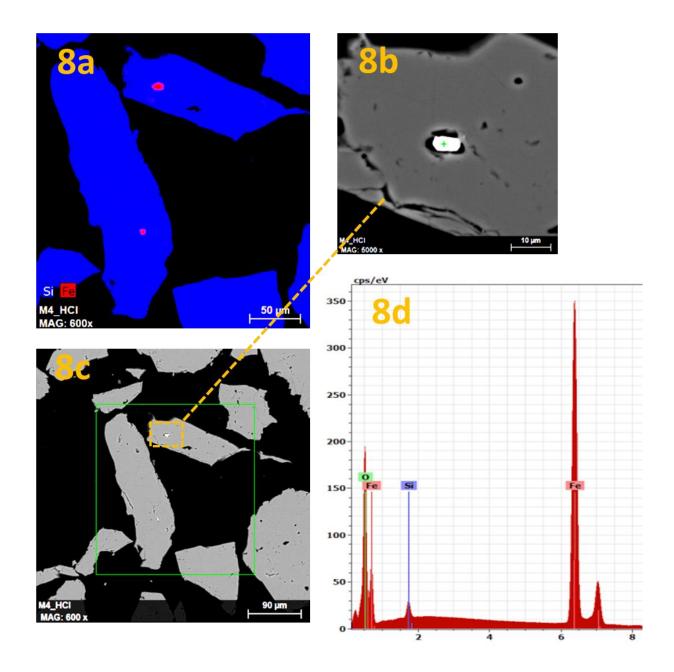
Figure 8: SEM-EDS analysis of M$_4$ (7M HCL, 107°C) showing residual iron containing solid inclusions by back scatted electron imaging (8a-c) and associated EDS spot analysis (8d)

In Figure 9 a decrepitation site identified in particle from sample RF$_1$ is shown, again with sodium rich remnant material around the edge.
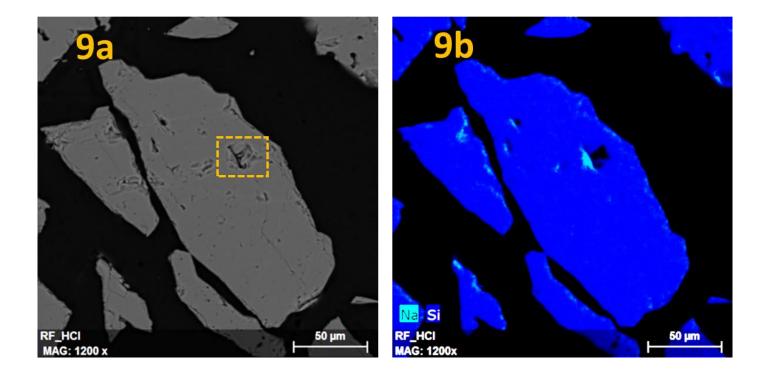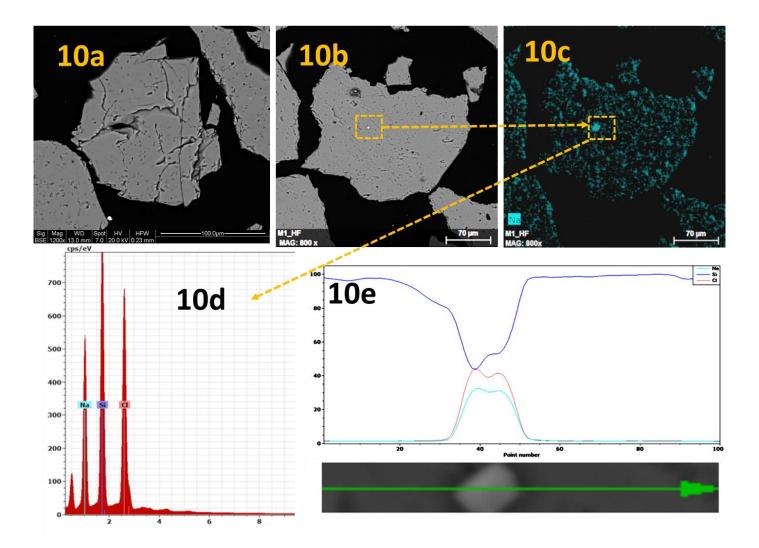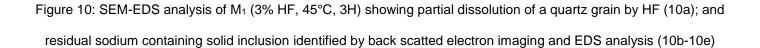
Figure 9: RF$_1$ (7M HCL, 107°C) showing a decrepitation site in a fragment analysed by SEM-EDX (9a) with identified residual sodium at its edges (9b)

The comparative effect of leaching with HF on M$_1$ is shown in Figure 10. It can be seen from image 10a that the HF solution has dissolved a proportion of the quartz itself, which is particularly evident at the edges and around fractures within the particles. Interestingly, remnant sodium was also identified occurring as a solid halite crystal within quartz matrix (10b-10e).

Figure 10: SEM-EDS analysis of M_1 (3% HF, 45°C, 3H) showing partial dissolution of a quartz grain by HF (10a); and residual sodium containing solid inclusion identified by back scatted electron imaging and EDS analysis (10b-10e)

3.5. STAGE FOUR – SINGLE MODE MICROWAVE CAVITY TESTS

A single mode cavity only supports a well-defined area of electric field at single principle frequency (or mode) (Metaxas and Meredith, 1983). By terminating the waveguide with an adjustable short circuit tuner, the incident and reflected waves can be superimposed on each other creating a single standing wave pattern. This creates areas within the cavity of high intensity, but spatially stable electric field. The previous work had shown that fluid inclusions could be selectively heated, but some inclusion sites remained intact, while others had decrepitated to form rings of smaller inclusions and scattered fluidic and solid debris. The objective of treating one of the multimode treated samples, was to determine if a high power single mode microwave system, can selectively heat the remaining impurity sites resulting in microfracture. This may then enable fluidic ingress on re-leaching and removal of the residual impurities. The applicator section of the experimental set-up is shown in Figure 11.
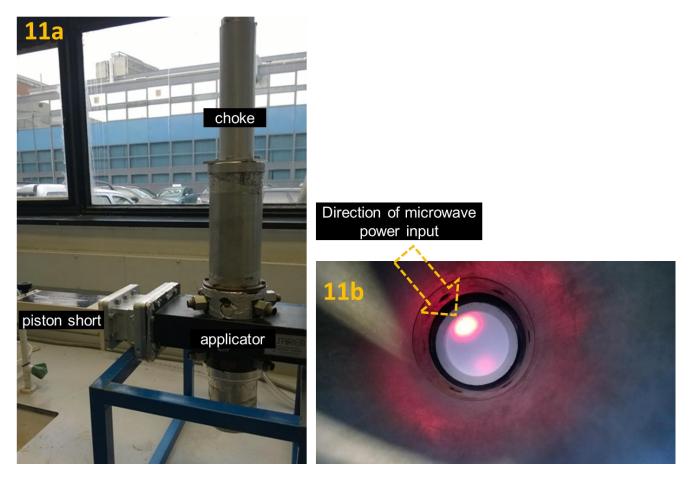
Figure 11: Experimental set up of the single mode applicator (11a) and from above down the choke during microwave treatment showing two 'hot spots' corresponding to areas of high electric field intensity within the quartz sample(11b)

The right-hand figure shows the sample held in a boronitride crucible during treatment. Note the two glowing hot-spots at the incident and rear face of the sample. This corresponds to the electric field maxima and thus the area which is heated strongest in the test sample (Shang et al., 2005). Both M_2 and M_3 (100g of each) from the stage three work, were heated in separate tests at 1.1kW for 14min and at this time, a maximum temperature of 450°C was reached, measured at the surface of the samples using an infra-red pyrometer. After cooling, they were then re-leached using the HF procedure (Table 6).

Table 6: ICP-AES elemental analysis of single mode treated samples and leached in HF (3% w/w, 45°C)

Sample ID	Leach Conditions	Elemental Composition (ppm)							
		Al	Ca	Cr	Fe	K	Na	Ti	Total
M_2	3% HF,	21 ± 1	2 ± 0.1	<0.2	3 ± 0.2	3 ± 0.1	12 ± 1	3 ± 0.1	44 ± 2
M_3	45°C	21 ± 1	2 ± 0.1	<0.2	5 ± 0.2	2 ± 0.1	12 ± 1	3 ± 0.1	44 ± 2

The single-mode tests yielded no further reductions in residual contamination levels. Despite measured temperatures (by infra-red pyrometer) of 450°C at the hotspot on the surface of the test sample during treatment and is considered in following section.

4. DISCUSSION

The preliminary tests were the most effective in terms of reduction in residual contaminant levels. Optical and SEM-EDS analysis of the treated material revealed that significant alteration of the bulk quartz was affected by exposure to microwave energy. This was particularly evident at micro-fluidic inclusion sites, where decrepitation resulted in explosive fracture of the contaminant site. In some cases, however, this was contained within the material resulting in a redisposition of the contaminant debris around its edge. This is supported by the re-leaching tests of the treated material ($M_1 - M_4$, RF_1) by boiling HCl and HF, where no improvement in purity was found. SEM-EDS analysis of the final product powders and optical analysis of the thin sections showed that larger inclusions in the size range 10 – 30um, readily decrepitated on microwave exposure, while those in the fine (2-5um) and ultra-fine (<2um) size ranges tended to persist to greater degree. Of particular interest is why a persistent level of sodium remains (ca. 10 - 12 ppm), irrespective of the treatment regime. This can be attributed to the presence of intact fine and ultra-fine inclusion sites after treatment and a combination of two mechanistic factors. The first is, in order for the contamination to be removed, that the decrepitation event must create a fracture pathway to the grain surface. If this is not achieved, then the leach solution cannot ingress into the grain and remove the contaminating debris. Evidenced in the SEM-EDS analysis in some cases is a redistribution of the inclusion fluid into even smaller inclusions by a partial melting and re-solidification of the decrepitation site. In order for an inclusion to fracture, the rate of heating must be sufficient to realise a pressure sufficient to exceed the confinement stress of the bulk quartz. The smaller the inclusion, the higher its surface area to volume ratio and therefore, the rate at which heat energy will dissipate to the surrounding quartz. It then follows that the smaller the inclusion the more difficult it is to fracture it, necessitating the use of increasingly higher treatment energies. This was evident by most of the larger inclusions being decrepitated, while the smaller ones persisted and remained largely unaltered across the treated samples. It is suggested that this is also an explanation as to why the single mode retreatment tests (section 3.5) did not reduce sodium levels in particular any more. Because the initial treatment had already fractured the largest inclusions and redistributed the associated debris, the 1.1kW of power applied was still not sufficient to fracture the smallest inclusions. Mapping inclusion size both before and after treatment within the same grain would support this explanation and would be valuable further information.

The second factor which may explain the persistence of sodium in the treated samples, is the fact that solid halite was identified, which appeared largely unaltered in treated samples (Figure 10). The dielectric properties of sodium chloride were measured at 2.45GHz by (Liu et al., 2013). For 0% moisture – which would be expected in the present case, the

values are dielectric constant $\varepsilon' = 2.418$, and the loss factor ($\varepsilon'' = 0.2084$). Solid halite is therefore classed as a 'lossy' material in that it readily heats in an electric field. In the microwave treatment of mineral ores it has been shown that microfracturing around grain margins occurs as the result of differential thermal expansion of the microwave absorbing grains when confined in a cold (microwave transparent) gangue (Batchelor et al., 2015). However, the effectiveness of this mechanism has been shown in other work to be dependent on the elastic modulus of the component phases (Djordjevic, 2014). In the present case, Young's elastic modulus of quartz is ca. 93 GPa (Djordjevic, 2014), and of halite ca. 3 GPa (Liang et al., 2012). Halite is therefore a very soft mineral confined by comparatively hard quartz. On heating of the halite grain in a microwave (or radio-wave) field, the resulting expansion will result in localised compression of the grain itself due to the confining stress of the quartz. It is suggested that the resulting strain is insufficient to fracture at the solid inclusion site. On cooling, the halite grain reverts to its near original dimensions and appears unaffected by the treatment and remains confined within the bulk quartz matrix, as has been observed (Figure 10).

In the stage two tests, these samples had a higher aluminium content (24 ± 2ppm) compared to stage one T_{10min} and T_{40min} (13 ± 0.7ppm) Subsequent analysis of the stage three acid leached samples (section 3.4) showed that these too had a generally higher aluminium content (24 ± 2ppm) content consistent with these being derived from the stage two material subsampled after the magnetic separation stage. Aluminium impurities are expected to reside as structural impurities in the quartz crystal and discrete feldspar phases within the whole pebbles. Overall the microwave effect was expected to have less direct effect on these, as alumina containing phases are comparatively low loss, that is, poor microwave absorbers compared to fluid inclusions. Microwave induced micro-fracture through the quartz will enhance leachate accessibility to the aluminium containing phases enhancing their removal. The stage one tests T_{10min} and T_{40min} had microwave treatment doses of 0.45 kWh/kg and ~1.8 kWh/kg. Stage two averaged a microwave treatment dose of 0.37kWh/kg and comparable to that delivered in the T_{10min} test. It is suggested that is this case use of the boronitride crucible and silica flour reduced the power density evolved in the pebbles themselves, ultimately inducing less microfractures in the pebbles and consequently less access of the leachate solutions to the aluminium containing phases. Quantification of microstructural damage as a function of microwave treatment energy; leach solution accessibility and residual aluminium content would be valuable further work.

It is suggested that further improvements in the upgrading of quartz can be achieved by evaluating the effect of a higher power microwave/RF system and the effect of feedstock preparation size. By optimising the grain size subject to microwave treatment, the evolution of micro-fracture to the grain surface can be enhanced and thereby increasing the effectiveness of subsequent leaching steps. The HF leaching trials, showed a significant reduction in residual aluminium, which could further be reduced using a stronger solution (only 3% was used in the present work).

Overall, microwave treatment of whole quartz pebbles, can selectively fracture containment sites, yielding reductions in residual contaminant levels of almost 25% compared to the non-microwaved untreated controls. Evaluating the processing as a whole, a total reduction in residual contamination of over 80% was achieved using simple and relatively environmentally friendly steps. In particular, removal of impurities associated with the elements calcium, sodium and potassium (those likely to be held in inclusion fluid) were reduced by 84; 78 and 50% respectively. Also significant was the reduction in residual aluminium containing impurities to an average of 12 ppm (multi-mode treatment for 40 min), compared to an average 19 ppm for the Ultra-High Pure Quartz product specification according to (Kogel, 2006). A summary of stage one to four compared to head grade composition is shown in Figure 12.
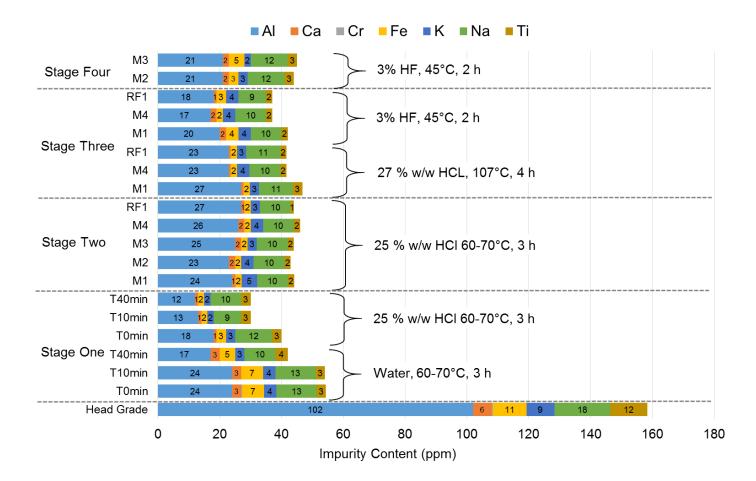

Figure 12: Summary comparison of residual elemental impurity content derived from stage one to four compared to head grade. Stage one – multimode cavity ; two – multimode cavity plus boronitride crucible and silica flour; three – re-leaching of stage two samples; four – single mode treatment and re-leaching of stage three samples with HF.

The refining steps presented in this work provide a viable alternative to traditional metallurgical routes to obtain solar grade silicon (Xakalashe and Tangstad, 2012). Further work using a single mode type applicators should be undertaken. The homogenous and relatively high electric field strengths characteristic of these types, may yield improvement in inclusion fracture.

The fine and ultra-fine size classes have been shown to be particularity resistant to microwave induced fracture. The corresponding increase in selective heating would be expected to enable fracturing in the difficult to treat fine and ultra-fine size-classes of inclusion. In this work only one source of quartz was evaluated. The process may be more amenable to other sources of quartz whose composition of fluid inclusions are higher in the larger sizes. Notwithstanding, the work presented shows that a microwave pre-treatment step is a simple and rapid method of securing commodity feedstocks for the production of Solar Grade Silicon (SoG) without having to rely on reject material from the semi-conductor industry.

5. CONCLUSIONS

The whole quartz pebbles evaluated in this study had a total impurity content of 158 ± 22ppm. Impurities were shown to predominantly reside in micro-fluidic inclusions and as solid inclusions within the quartz matrix itself. Using a combination of microwave treatment of the whole quartz pebble in a multimode cavity, crushing and milling, high intensity wet magnetic separation, and acid leaching, in the best case reduced the total residual impurities to 30 ± 4 ppm (or 80%). Significant is the targeted reduction in residual elemental impurity content, associated with micro-fluidic inclusion sites, containing calcium; potassium and sodium of 84; 78; and 50 % respectively. Also, a statistically significant reduction in residual aluminium phases was also observed of 102 ± 14 ppm (in as received pebbles) to 12 ppm (multi-mode treatment, 40 minutes) and is below the grade limit for IOTA Ultra-High Pure Quartz. The final product quartz has and purity intermediate between metallurgical and solar grade silicon.

Considering the microwave step alone, this yielded a reduction of 10ppm (or 25%) compared to the control set subject to size reduction, magnetic separation and leaching alone, which gave a residual impurity level of 41 ± 6ppm. This was attributed to targeted decrepitation of micro-fluidic sites within the quartz matrix by selectively heating the inclusion fluid. The resulting fracture of the site then allows subsequent processing steps to remove the impurities.

The persistence of residual impurities were found to be the result of re-deposition of inclusion debris around the fracture site and persistent solid inclusions that were less amenable to microwave treatment. The initial multimode cavity microwave treatments were shown to be the most effective in terms of upgrading the quartz pebbles. Treatment times of only 10min in a relatively simple system were required. Residual impurity levels remained constant when retreated under more aggressive leaching conditions (3% HF).

This work has shown that natural quartz pebbles can be upgraded through a combination of microwave treatment, magnetic and chemical refinement to produce a viable feedstock for the subsequent production of solar grade silicon.

REFERENCES

Ali, A., Bradshaw, S., 2011. Confined particle bed breakage of microwave treated and untreated ores. Minerals Engineering 24, 1625-1630.

Amankwah, R., Khan, A., Pickles, C., Yen, W., 2005. Improved grindability and gold liberation by microwave pretreatment of a free-milling gold ore. Mineral Processing and Extractive Metallurgy 114, 30-36.

Barker, C., Robinson, S., 1984. Thermal release of water from natural quartz. Am. Mineral.;(United States) 69.

Batchelor, A., Ferrari-John, R., Dodds, C., Kingman, S., 2016. Pilot scale microwave sorting of porphyry copper ores: Part 2–Pilot plant trials. Minerals Engineering 98, 328-338.

Batchelor, A., Jones, D., Plint, S., Kingman, S., 2015. Deriving the ideal ore texture for microwave treatment of metalliferous ores. Minerals Engineering 84, 116-129.

Bodnar, R.J., 2003. Reequilibration of fluid inclusions. Fluid inclusions: Analysis and interpretation 32, 213-230.

Bye, G., Ceccaroli, B., 2014. Solar grade silicon: Technology status and industrial trends. Solar Energy Materials and Solar Cells 130, 634-646.

Delannoy, Y., 2012. Purification of silicon for photovoltaic applications. Journal of Crystal Growth 360, 61-67.

Djordjevic, N., 2014. Recovery of copper sulphides mineral grains at coarse rock fragments size. Minerals Engineering 64, 131-138.

Drouiche, N., Cuellar, P., Kerkar, F., Medjahed, S., Boutouchent-Guerfi, N., Ould Hamou, M., 2014. Recovery of solar grade silicon from kerf loss slurry waste. Renewable and Sustainable Energy Reviews 32, 936-943.

Ferrari-John, R., Batchelor, A., Katrib, J., Dodds, C., Kingman, S., 2016. Understanding selectivity in radio frequency and microwave sorting of porphyry copper ores. International Journal of Mineral Processing.

Frankl, P., Nowak, S., Gutschner, M., Gnos, S., Rinke, T., 2010. International energy agency technology roadmap: solar photovoltaic energy.

Götze, J., Plötze, M., Graupner, T., Hallbauer, D.K., Bray, C.J., 2004. Trace element incorporation into quartz: a combined study by ICP-MS, electron spin resonance, cathodoluminescence, capillary ion analysis, and gas chromatography. Geochimica et Cosmochimica Acta 68, 3741-3759.

Hughes, E., 2013. High Purity Quartz - A Cut Above, Industrial Minerals.

Jones, D., Lelyveld, T., Mavrofidis, S., Kingman, S., Miles, N., 2002. Microwave heating applications in environmental engineering—a review. Resources, conservation and recycling 34, 75-90.

Junior, I.P., Pereira, M.S., dos Santos, J.M., Duarte, C.R., Ataíde, C.H., Panisset, C.M.d.Á., 2015. Microwave remediation of oil well drill cuttings. Journal of Petroleum Science and Engineering 134, 23-29.

Kappe, C.O., Dallinger, D., 2006. The impact of microwave synthesis on drug discovery. Nature Reviews Drug Discovery 5, 51.

Kendrick, M., Phillips, D., Miller, J.M., 2006. Part I. Decrepitation and degassing behaviour of quartz up to 1560 C: analysis of noble gases and halogens in complex fluid inclusion assemblages. Geochimica et Cosmochimica Acta 70, 2540-2561.

Kendrick, M.A., Burnard, P., 2013. Noble gases and halogens in fluid inclusions: A journey through the Earth's crust, The noble gases as geochemical tracers. Springer, pp. 319-369.

Kitchen, H.J., Vallance, S.R., Kennedy, J.L., Tapia-Ruiz, N., Carassiti, L., Harrison, A., Whittaker, A.G., Drysdale, T.D., Kingman, S.W., Gregory, D.H., 2013. Modern microwave methods in solid-state inorganic materials chemistry: from fundamentals to manufacturing. Chemical reviews 114, 1170-1206.

Kogel, J.E., 2006. Industrial minerals & rocks: commodities, markets, and uses. SME.

Liang, W., Zhang, C., Gao, H., Yang, X., Xu, S., Zhao, Y., 2012. Experiments on mechanical properties of salt rocks under cyclic loading. Journal of Rock Mechanics and Geotechnical Engineering 4, 54-61.

Liu, C., Zhang, L., Peng, J., Qu, W., Liu, B., Xia, H., Zhou, J., 2013. Dielectric properties and microwave heating characteristics of sodium chloride at 2.45 GHz. High Temperature Materials and Processes 32, 587-596.

Lynch, D., 2009. Winning the global race for solar silicon. JOM 61, 41-48.

Marland, S., Han, B., Merchant, A., Rowson, N., 2000. The effect of microwave radiation on coal grindability. Fuel 79, 1283-1288.

Metaxas, A.a., Meredith, R.J., 1983. Industrial microwave heating. IET.

Pizzini, S., 2010. Towards solar grade silicon: Challenges and benefits for low cost photovoltaics. Solar energy materials and solar cells 94, 1528-1533.

Roedder, E., Ribbe, P., 1984. Fluid inclusions. Mineralogical Society of America Washington, DC.

Safarian, J., Tranell, G., Tangstad, M., 2012. Processes for upgrading metallurgical grade silicon to solar grade silicon. Energy Procedia 20, 88-97.

Santos, M.F., Fujiwara, E., Schenkel, E.A., Enzweiler, J., Suzuki, C.K., 2015. Processing of quartz lumps rejected by silicon industry to obtain a raw material for silica glass. International Journal of Mineral Processing 135, 65-70.

Sarti, D., Einhaus, R., 2002. Silicon feedstock for the multi-crystalline photovoltaic industry. Solar energy materials and solar cells 72, 27-40.

Shang, H., Snape, C., Kingman, S., Robinson, J., 2006. Microwave treatment of oil-contaminated North Sea drill cuttings in a high power multimode cavity. Separation and purification technology 49, 84-90.

Shang, H., Snape, C.E., Kingman, S.W., Robinson, J.P., 2005. Treatment of oil-contaminated drill cuttings by microwave heating in a high-power single-mode cavity. Industrial & engineering chemistry research 44, 6837-6844.

Xakalashe, B.S., Tangstad, M., 2012. Silicon processing: from quartz to crystalline silicon solar cells. Chem Technol, 32-37.